Tropical Journal of Pharmaceutical Research October 2023; 22 (10): 2087-2097
ISSN: 1596-5996 (print); 1596-9827 (electronic)

Available online at http://www.tjpr.org
http://dx.doi.org/10.4314/tjpr.v22i10.10

Original Research Article

Effect of gold nanocomposite bearing HIF-1α siRNA on radiotherapy in nasopharyngeal carcinoma cell

Haosheng Zhang*, Fangzheng Zhou
Department of Radiation Oncology, Shenzhen Luohu People's Hospital, The Third Affiliated Hospital (The Affiliated Luohu Hospital) of Shenzhen University, Shenzhen Luohu Hospital Group, 47 Youyi Road, Luohu District, Shenzhen 518020, People's Republic of China

For correspondence:* ***Email:* *m19210480506@163.com*

Sent for review: 17 June 2023 *Revised accepted: 7 October 2023*

Abstract

Purpose: *To investigate the effect of gold nanocomposite carrying hypoxia-inducible factor-1α (HIF-1α) siRNA on radiosensitivity of nasopharynx cancer (NPC) cells.*
Methods: *Gold nanocomposite (AuNRs-(PEI-PEG)/RGD) or (AuPPR) was first synthesized and its cytotoxicity was evaluated. Then, the expression of HIF-1α in hypoxic NPC cells was assessed. In addition, the radiation sensitivity of AuPPR bearing HIF-1α siRNA on the cells was examined under x-ray exposure.*
Result: *Gold nanocomposite (AuPPR) carrying HIF-1α siRNA (AuPPR-HIF-1α siRNA) significantly down-regulated HIF-1α expression. Under irradiation treatment, AuPPR-HIF-1α siRNA significantly enhanced apoptosis of NPC cells by 33.76 ± 3.65 %, when compared to the control and simple AuPPR group (22.5 ± 4.16 %, $p < 0.01$). Furthermore, cell cycle was significantly blocked in the sub-G1 phase in AuPPR-HIF-1α siRNA radiotherapy groups, indicating severe cell damage.*
Conclusion: *This study has demonstrated that AuPPR-HIF-1α siRNA is effective in improving the radiosensitivity of nasopharyngeal carcinoma cells under hypoxia, and therefore can potentially be used to improve the radiotherapy of this carcinoma.*

Keywords: *Gold nanoparticles, Nasopharynx cells, Cancer, Hypoxia, Hypoxia-inducible factor-1α, Radiation susceptibility, Radiotherapy, Radiosensitivity*

Tropical Journal of Pharmaceutical Research is indexed by Science Citation Index (SciSearch), Scopus, Web of Science, Chemical Abstracts, Embase, Index Copernicus, EBSCO, African Index Medicus, JournalSeek, Journal Citation Reports/Science Edition, Directory of Open Access Journals (DOAJ), African Journal Online, Bioline International, Open-J-Gate and Pharmacy Abstracts

INTRODUCTION

There is a high frequency of nasopharynx cancer (NPC) in Asia. Radiotherapy is an important treatment for most patients with NPC. The five-year survival of NPC subjects treated with radiotherapeutic strategy is approximately 94 % [1]. Nonetheless, the effectiveness of this treatment mode in patients with nasopharyngeal carcinoma is significantly related to the radiosensitivity of nasopharyngeal carcinoma cells, which affects the prognosis in patients. Radiosensitivity of cancer cells is associated with hypoxia in their immediate vicinity, which decreases radiation sensitivity and suppresses apoptotic changes in cancer cells, resulting in decreased curative effects [2]. Earlier investigations revealed that hypoxia-inducible factor-1α (HIF-1α) is a key transcription factor

involved in tumor adaptation to hypoxia [3]. In a solid tumor such as NPC, tumor cells exist in a micro-environment of hypoxia, with HIF-1α expression on the increase, thereby increasing the resistance of tumor cells to radiotherapy [4]. Therefore, inhibition of HIF-1α expression may effectively improve the radio-sensitivity of hypoxic nasopharyngeal carcinoma cells.

The RNAi has small interfering RNA (siRNA) that reduces HIF-1α mRNA expression. Nevertheless, due to negative charge on HIF-1α siRNA, it is difficult for it to pass through cell membranes thus affecting the delivery of HIF-1α siRNA [5]. Current research, therefore, is focused on how to safely and effectively deliver HIF-1α siRNA into cells.

The rapid development of research on gold nanomaterials has provided new approach to addressing the radio-sensitivity of hypoxic tumor cells. The size of gold nanomaterials is smaller than 100 nm, and they have chemical inertness and good bio-compatibility. It has been reported that gold nanoparticles (AuNRs) may be combined with positive cationic polymers like polyethyleneimine-polyethylene glycol copolymer (PEI-PEG) and nucleic acid molecules (DNA and RNA) [6]. Under certain energy irradiation, AuNRs produce secondary electrons and reactive oxygen species (ROS), increase DNA damage of tumor cells, and improve the sensitivity of hypoxic tumor cells to radiotherapy [7]. It was first reported in 2004 that nanogold sensitizes tumors to the effect of radiation [8]. Then, in 2017, Chang *et al* [9] designed gold and selenium nanocomposites for radiotherapy of cancer. Figure 1 A is a scheme that depicts the radio-sensitization mechanism of AuNRs under irradiation. Polyethyleneimine (PEI) is a cationic polymer with surface chemical groups that modify gold nanorods and electrostatically adsorb to a negatively charged nucleic acid molecule such as siRNA. In addition, PEI, a typical representative cationic polymer gene carrier, has a unique "proton-sponging effect" that protects nucleic acid molecules from nuclease-catalyzed degradation in the cytoplasm [10]. However, PEIs of high molecular weights (above 25 kDa) exert greater toxic effects on cells, resulting in damage to normal tissue cells. On the other hand, the transfection efficiency of low molecular weight PEIs, e.g., 1.8 kDa, is low [15]. This limits wide application of these PEIs. The combination of polyethylene glycol (PEG) with PEI changes the chemical structure of the cationic polymer, thereby reducing its biological toxicity. In this study, PEG was combined with low molecular weight (1.8 kDa) PEI so as to reduce the cytotoxicity of the nanomaterial. The cationic polymer (PEI-PEG) is readily metabolized to CO_2 and H_2O, which are easily eliminated from the body to avoid toxic accumulation [10]. The mechanism of action of gold nano-composites within hypoxic cells is depicted in a scheme in Figure 1 B.

It has been reported that the integrin receptor αvβ3 is specifically present in the membranes of cancer cells, but it is hardly found on normal membrane surfaces. The arginine-glycine-aspartate tripeptide (Arg-Gly-Asp, RGD) specifically recognizes αvβ3 receptor on the tumor cell membrane [11]. A study has demonstrated that nanoparticles modified by RGD enhanced endocytosis of tumor cells, thereby improving transfection efficiency and targeting. Therefore, PEI-PEG)/RGD copolymers have the potential to carry HIF-1α siRNA with low toxicity, efficient gene transfection efficiency, and good targeting.

This study aimed to investigate whether AuNRs bearing HIF-1α siRNA {AuNRs-(PEI-PEG)/RGD-HIF-1α siRNA} (AuPPR-HIF-1α siRNA) effectively enhances the radio-susceptibility of hypoxic NPC cells and improves radiotherapeutic effects in NPC patients.

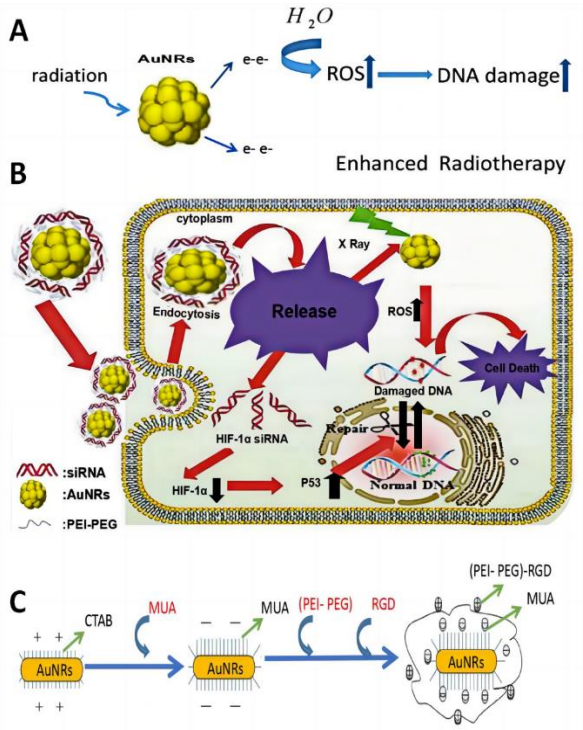

Figure 1: (A) Scheme illustrating the mechanism of radio-sensitization of gold nanoparticles under photon irradiation, (B) Actions of gold nano-composite carrying HIF-1α siRNA after entering the hypoxic cells, (C) Steps in the synthesis of AuNRs-(PEI-PEG)/RGD

EXPERIMENTAL

Preparation of AuNRs-(PEI-PEG)/RGD

The AuNRs-CTAB was synthesized at Shenzhen Institute of Advanced Technology of Chinese Academy of Sciences using the crystal growth method. Subsequently, mercapto-undecanoic acid (MUA) was used to displace cetyltrimethylammonium bromide (CTAB) with a positive potential, resulting in generation of AuNRs-MUA with a negative surface potential. The MUA enhanced the binding of AuNRs to the cationic polymer PEI-PEG [12].

The mixture of mPEG-Sc and PEI-Et (1.8 kDa) was added to an aqueous solution of sodium hydrogen carbonate in proportions of 4:1 - 8:1, stirred at room temperature for 24 h, and then set aside for 2 h to purify the cationic copolymer (PEI-PEG). Subsequently, the cationic copolymer (PEI-PEG) was added to the AuNRs-MUA solution under ultrasonic vibration, and the mixture was incubated for 2 h, followed by centrifugation at 8000 rpm for 15 min to remove unbound reactants. This process yielded gold nanorod carrier complex, i.e., AuNRs-(PEI-PEG). In addition, AuNRs-(PEI-PEG)/RGD (AuPPR) was carefully produced by combining the carboxyl group at the end of RGD with the PEI. The concentration of the AuPPR product was adjusted to 20 µg/mL, prior to use. The steps followed in the synthesis of AuPPR are shown in Figure 1 C. The products obtained were characterized using an electron microscope.

Cytotoxicity of different modifiers of AuNRS

The liver cells were selected for toxicity testing as the liver is the largest organ involved in metabolism. The cells were cultured in a medium containing 100 µmol/L of $CoCl_2$ which is often used to induce hypoxia *in vitro* to mimic the hypoxic environment of cells. After cell counting, 100 µL of a suspension containing about 1000 - 10000 cells in logarithmic growth was put inside every well in a 96-well plate, followed by 24-h culturing. Thereafter, the cells, which were all treated with cobalt chloride ($CoCl_2$), were divided into 6 experimental groups viz: control (treated with sterile saline), AuNRs-CT AB, AuNRs-MUA, AuNRs-PEI, AuNRs-(PEI-PEG) and AuPPR groups. The treatments were given at four final graded concentrations for each group: 10, 20, 30 and 40 µg/mL. After 48 h of culturing in each group, 20 µL of CCK-8 solution was put into every well. Cell culturing was terminated 2 h later, and absorbance (A) was read at 450 nm using a microplate reader. The cell viability was calculated using Eq 1.

$$\text{Cell viability (\%)} = \{(Ae-Ab)/(Ac-Ab)\}100 \quad \ldots. (1)$$

where Ae is the absorbance of experimental well, Ab is the absorbance of blank well and Ac is the absorbance of control well.

Potential of AuPPR to bind to HIF-1A siRNA

Since AuPPR is adsorbed to negatively-charged siRNA nucleic acids through surface cationic polymer (PEI-PEG), a gel electrophoresis experiment was used to determine the potential of AuPPR to bind to FAM-siRNA. For this purpose, 20 µM siRNA solution in diethylpyrocarbonate (DEPC) water was mixed with the AuPPR nanoparticles (20 µg/mL; this concentration was chosen based on the results of cytotoxicity test) at seven volume ratios of 2:1, 1:1, 1:2, 1:3, 1:4, 1:5, and 1:6 (siRNA: AuPPR nanoparticles). The siRNA solution sample (20 µM) and DEPC (control) were diluted to the same concentration gradients as above and then left to stand for 30 min as control group. Using a 1 % agarose gel, 20 µL of each group of the above experimental and control groups were electrophoresed at a voltage of 110 V for 20 min.

Transfection with AuPPR -HIF-1A siRNA

Cells treated with $CoCl_2$ in order to simulate hypoxic environment were assigned to four groups: HIF-1α siRNA and AuNRs-(PEI-PEG)-HIF-1α siRNA groups, as well as AuPPR-HIF-1α siRNA group and AuPPR-NC siRNA group (NCsiRNA/negative control group). The cells were seeded in a 6-well cell culture plate at a density of 5 - 10 $\times 10^4$ cells/well and cultured for 24 h in a medium containing 100 µmol/L of $CoCl_2$ without antibiotics. When the cell density increased to 50 – 70 %, the medium containing cobalt chloride was replaced with normal medium. The above groups (20 µg/mL, fluorescence-labeled) were mixed with the medium in a 1:4 volume ratio in the dark (this ratio was selected based on the results of gel electrophoresis experiment). After standing undisturbed for ½ h in darkness, it was filtered and the cells were seeded in the above 6-well plate, followed by a 4-h incubation. After rinsing in PBS, a 20-min cell fixation in 4 % paraformaldehyde was done. Thereafter, the cells were incubated in a DAPI staining incubator for 10 min, and washed at least thrice with PBS to remove FAM-siRNA on the surface of the plate and cell surface. The phenomenon

of transfection and intracellular distribution were examined under an inverted fluorescence microscope, and the population of cells in every field of view (Tc) was calculated with a cell counting plate. Finally, the number of fluorescent cells (Fc) was computed. Transfection efficiency (TE) was calculated using Eq 2.

TE (%) = (Nc/Tc)100 …… (2)

Western blotting

This test was used to determine the effect of transfection. After transfection for 48 h, the medium was discarded, and the cells were washed with PBS. Total protein was extracted from cells in each group using RIPA buffer. Cells adhering to the bottom wall of the culture flask were scraped to ensure efficient cell lysis. Lysates were subjected to centrifugation to obtain total protein extract. Proteins were resolved on 10 % SDS-polyacrylamide gel electrophoresis, followed by electro-transfer to PVDF membranes which were thereafter blocked by incubation with 5 % fat-free milk for 1 h at laboratory temperature. After rinsing the membranes thrice with PBST, they were incubated on a shaker for 12 h with the 1^{o} immunoglobulins for HIF-1α (diluted 1:1000) and β-actin (diluted 1:1000) at 4 °C. After rinsing 3 times with 1 × PBST, the membranes were incubated with secondary antibody (1:1000) for 80 min at room temperature on a shaker. The bands were subjected to enhanced chemiluminescent analysis with SuperSignal for 1 min, followed by imaging using fluorescence imager.

Determination of relative ROS content

Four groups of cells comprising control group (treated with physiological saline), AuNRS, AuPPR-NCsiRNA, AND AuPPR-HIF-1A siRNA2 groups were set up (three sets of siRNA sequences were designed in the study, with siRNA2 being the optimal sequence). hypoxia was simulated in all groups with $COCl_2$ treatment. The cells in each group were cultured for 24 h. then, some of the culture wells in each group were irradiated with a single dose (4 gy) of photons. However, some of the wells were non-irradiated. After irradiation, the cells were adjusted to a concentration of 1×10^6 cells/well. then, 10 μm DCFH-DA was pipetted into six-well plate and incubated for 0.5 h at 37°c in a 5 %-co_2 incubator. During the period, the six-well plate was shaken every 3 - 5 min to make the probe and the cells fully interact. The cells were washed three times with serum-free medium or warmed in pbs solution in the dark to eliminate DCFH-DA that did not enter the cells. The ROS in each group of cells was determined using a flow cytometer.

Determination of cell cycle and apoptosis of CNE-2 cells

Cells were cultured for 24 h after irradiation, after which they were stained with DCFH-DA in the dark, using same method as described above. Following incubation for 10 - 20 min, analysis was done using a flow cytometer after 1 h. The cell cycle changes and apoptosis ratios in each group were analyzed.

Statistical analysis

Data are presented as mean ± standard deviation (SD). Analysis of variance (ANOVA) and *t*-test for statistical significance were performed using SPSS 13.0 software. Statistical significance was assumed at $p < 0.05$.

RESULTS

Gold nanoparticle carrier composite (AuPPR)

After modification, the cationic polymer-coated gold nanorods were examined under an electron microscope. As shown in Figure 2 A, gold nanorod carrier complex (AuPPR) appeared under an electron microscope (x20) with long diameter of about 40 - 50 nm and short diameter of 10 - 15 nm. The average particle distribution radius measured with Dynamic Lighting Scattering (DLS) was 26.02 ± 0.744 nm. During the modification of AuNRs, the zeta potential changed, as expected. The surface of the positively charged group of AuNRs-CTAB was replaced with the anionic group MUA. The zeta potential changed from a positive potential to a negative potential. After the cationic polymer (PEI-PEG) was modified, the potential was converted to a positive status (Figure 2 B). The zeta potential of AuNRs (48.71 ± 3.99 mV) and that of modified AuPPR (43.94 ± 6.95 mV) were comparable, as depicted in Figure 2 C. During the modification of AuNRs, there was no change in the transverse surface plasmon resonance (TSPR) absorption peak (the first peak) in the UV spectra. However, there was a change in the long-wave longitudinal surface plasmon resonance (LSPR) absorption peak (the second peak), as shown in Figure 2 D. The phenomenon of UV redshift in the LSPR indicates that the long diameter of the nanoparticles was prolonged during the

modification of AuNRs. These data indicate that AuNRs were successfully modified.

Cytotoxicity of modified AuNRs

The cytotoxic effects of different modified forms of AuNRs were evaluated. In WRL68 hepatocytes and human NPC cells, cell viability decreased with increase in the concentration of each nano-preparation (F_{WRL68} = 77.2, p < 0.01; F_{CNE-2} = 54.2, p < 0.01). In particular, AuNRs-CTAB was highly toxic to both hepatocytes and CNE-2 cells, followed by AuNRs-PEI, while AuNRs-(PEI-PEG) and AuPPR were less toxic to hepatocytes and CNE-2 than AuNRs-CTAB and AuNRs-PEI. The cytotoxicity experiments showed that the biological toxicity was significantly reduced by the modified gold nanorod carrier complex (AuPPR). In addition, when the concentration of AuPPR was 20 µg/mL, the hepatocytes still had high cell viability (82.03 ± 1.98 %). These results are shown in Figure 3 A. Therefore, AuPPR was used at the concentration of 20 µg/mL for subsequent experiments.

HIF-1α siRNAy was fully bound to AuPPR

Gel electrophoresis experiment was used to determine the siRNAs bound to AuPPR. Compared with the control group, the nucleic acid in AuPPR-HIF-1α siRNA group could not be separated from AuPPR by electrophoresis at a certain concentration (ratio of 1:4 or higher), indicating that siRNA was completely adsorbed on AuPPR. These results are shown in Figure 3 B.

RGD-modified AuPPR improved the transfection efficiency of HIF-1α siRNA in NPC cells

To evaluate the transfection efficiency of AuPPR-bearing siRNA, fluorescence experiments were performed. The results revealed that simple HIF-1α siRNA hardly entered cells without the carrier. In contrast, the transfection efficiency of AuNRs-PEI-PEG without RGD was approximately 42 ± 7.9 %, which was increased when compared to the simple HIF-1α siRNA group. The transfection efficiencies of AuPPR with RGD bearing HIF-1α siRNA and NCsiRNA (negative control group) were about 84 ± 8.2 % and 85 ± 12.2 %, respectively, as shown in Figure 4. These results demonstrate that AuPPR may be an ideal nanomaterial for transfecting nucleic acids, as it efficiently carries HIF-1α siRNA into cells. In addition, the impact of HIF-1α siRNA on HIF-1α protein level was evaluated with western blotting. The results of western blotting showed that the AuPPR-HIF-1α siRNA2 group effectively reduced the expression of HIF-1α protein (Figure 5). These results revealed that AuPPR effectively carried HIF-1α siRNA2 into the cells and effectively silenced the mRNA and protein expression levels of HIF-1α.

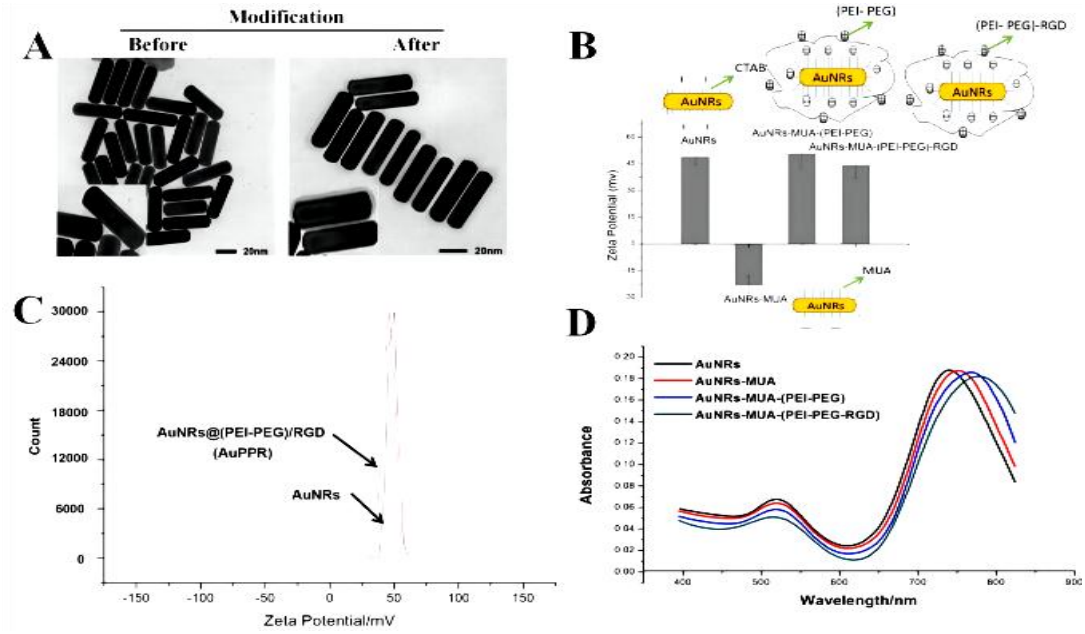

Figure 2: Characterization and effects of AuNRs. (A) Gold nanoparticles as seen under the electron microscope (x20), before modification or after modification, (B & C) Changes in zeta potential during the modification of AuNRs, (D) Changes in UV absorption spectra during AuNRs modification

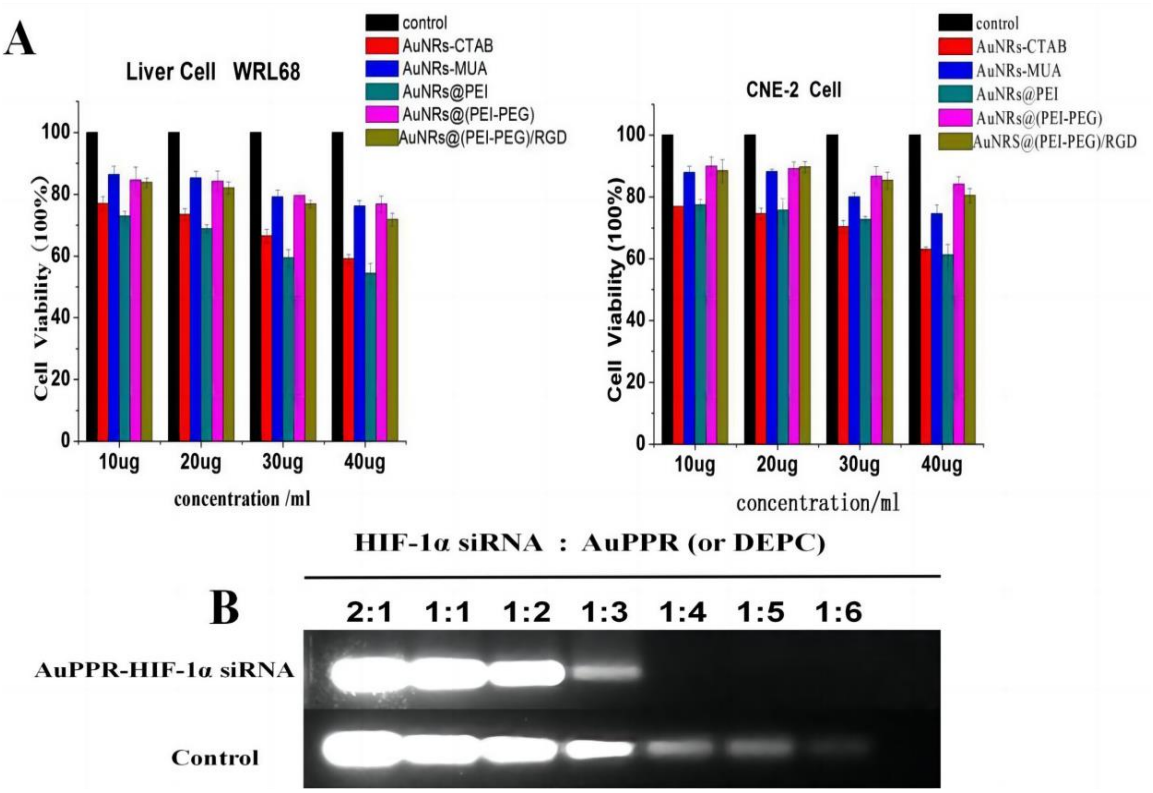

Figure 3: Changes in cytotoxicity during the modification of AuNRs, and determination of binding of HIF-1α siRNA to AuPPR. (A) Impact of various AuNR modifications on the proliferation of hepatic cells and the NPC cells, (B) Gel electrophoresis showing the binding of siRNA to AuPPR at different concentrations in the experimental and control groups. (Control group: siRNA: DEPC water; experimental group: siRNA: AuPPR)

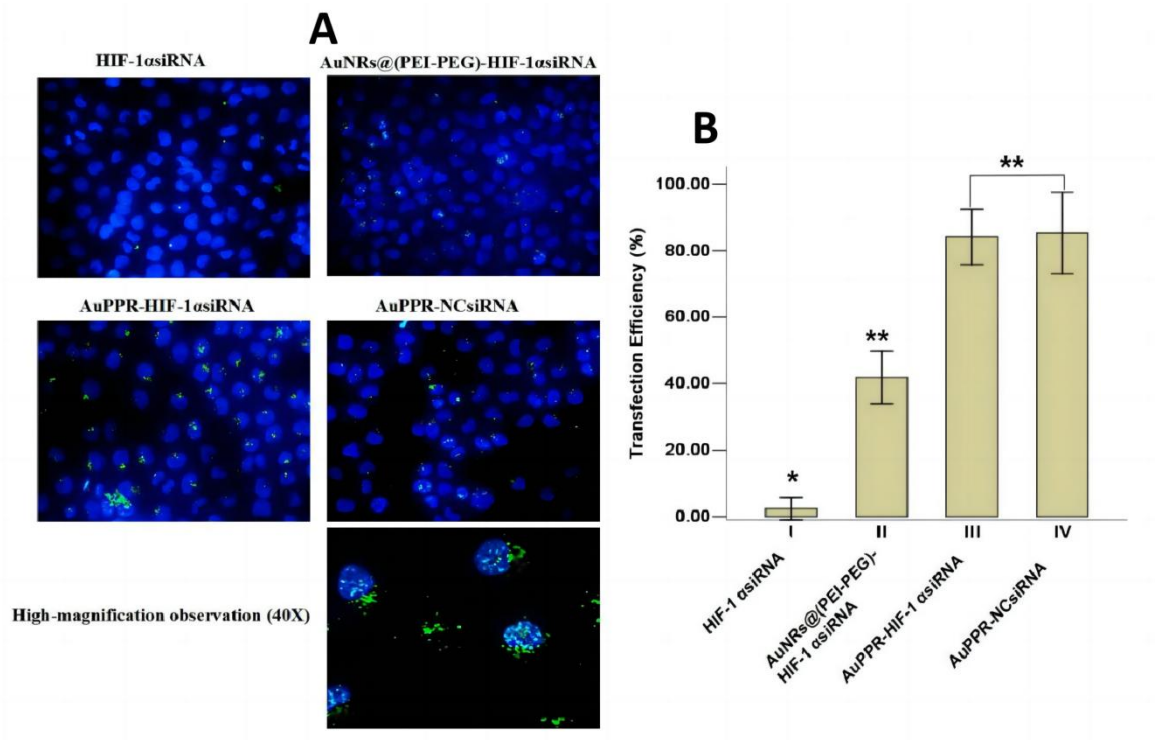

Figure 4: Transfection efficiency of nanocarrier (AuPPR). (A) Cell transfection under a fluorescence microscope. (B) Comparison of cell transfection statistical plots

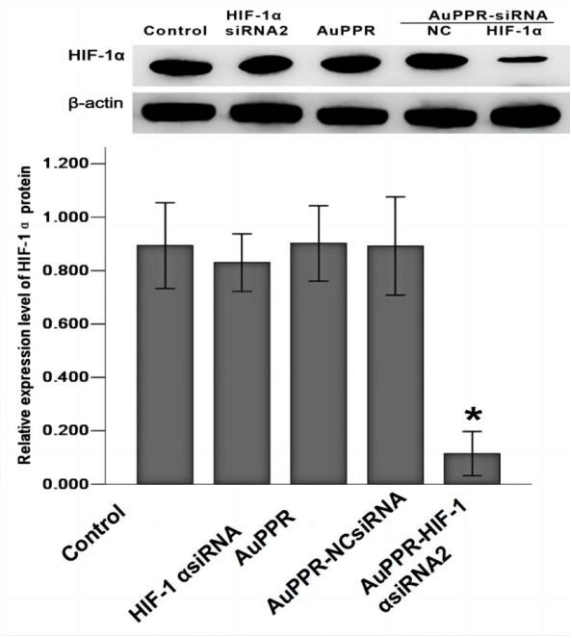

Figure 5: Relative expression level of HIF-1α. AuPPR-HIF-1α siRNA2 effectively inhibited the expression of HIF-1α protein

Irradiation of AuNRs accentuated ROS levels

The ROS are important factors in the radiosensitivity of tumors. Therefore, we evaluated the effect of gold nanoparticles on ROS production under irradiation conditions to explore the relevant sensitization mechanism [10]. There was no significant elevation in ROS in each group in the absence of irradiation. In contrast, ROS levels increased in all groups after irradiation. Compared with the control group, simple AuPPR group, AuPPR-NCsiRNA group and AuPPR-HIF-1α siRNA2 group showed marked increases in ROS production under irradiation conditions. Furthermore, compared with simple AuPPR and AuPPR-NCsiRNA groups, there was a slight increase in the amount of ROS produced in the AuPPR-HIF-1α siRNA2 group after irradiation (Figure 6).

AuPPR-HIF-1α siRNA2 improved the radiosensitivity of tumor cells

Flow cytometry was used to investigate the effect of AuPPR-HIF1αsiRNA2 on the cell cycle and apoptosis. In the absence of X-ray irradiation, AuPPR-HIF-1α siRNA2 significantly blocked the G2/M phase of CNE-2 cell (Figure 7 B). After irradiation, the CNE-2 cells showed different degrees of G2/M phase arrest in all groups (Figure 7 B). Cells in the AuPPR-HIF-1α siRNA2-irradiation group had a significant sub-G1 peak, indicating evidence of severe apoptosis and necrosis. Moreover, in the absence of X-ray irradiation, the apoptosis rates in the AuPPR group (5.17 ± 0.31 %), AuPPR-NCsiRNA group (4.87 ± 0.40 %) and AuPPR-HIF-1α siRNA2 group (7.90 ± 0.66 %) were increased, when compared with that in the control group (3.66 ± 0.31 %). These data are presented in Figure 7 A. Apoptosis rate was significantly higher in AuPPR-HIF-1α siRNA2 group than in the remaining three groups. There was no significant difference in the rate of apoptosis between the AuPPR group and the AuPPR-NCsiRNA group. The degree of apoptosis of all groups increased to varying degrees after X-ray radiation.

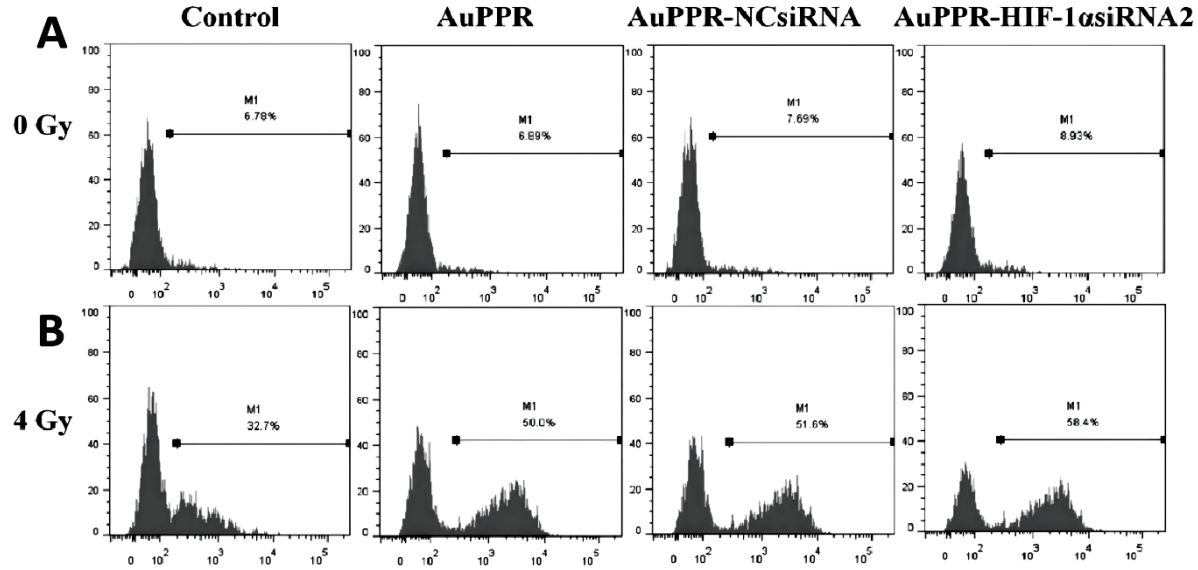

Figure 6: ROS levels of cells treated with or without irradiation. (A) ROS content without irradiation, (B) ROS content under irradiation (4 Gy)

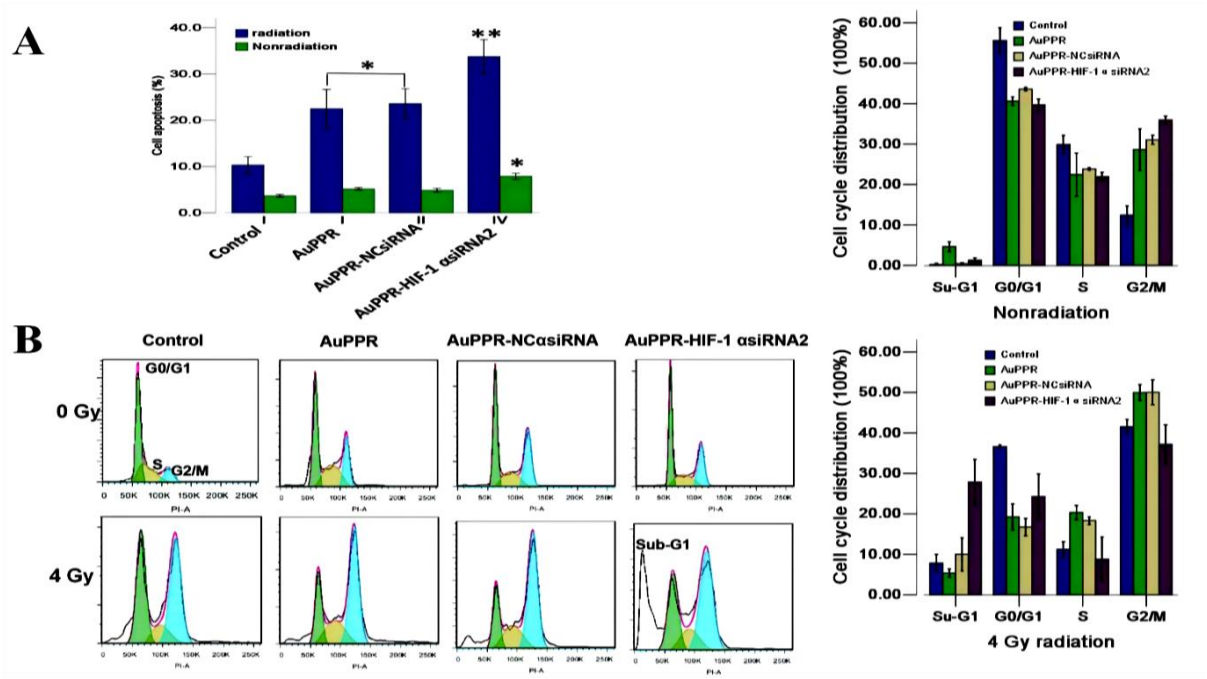

Figure 7: AuPPR-HIF-1α siRNA2 enhanced radio-sensitivity of cancer cells *in vitro*. (A) Apoptosis rate of CNE-2 cells treated with or without irradiation, (B) Cell cycle distribution. *P < 0.05, **p < 0.01 (AuPPR-HIF-1α siRNA group vs control group, AuPPR group or AuPPR-NCsiRNA group)

Compared with the degree of apoptosis in the irradiation control group (10.33 ± 1.79 %), the apoptosis rates in the AuPPR-irradiation group (22.5 ± 4.16 %), AuPPR-NCsiRNA-irradiation group (23.6 ± 3.17 %) and AuPPR-HIF-1α siRNA2-irradiation group (33.76 ± 3.65 %) were significantly increased. In particular, the apoptosis rate was significantly higher in the AuPPR-HIF-1α siRNA2-irradiation group than in the AuPPR-irradiation group as well as the AuPPR-NCsiRNA-irradiation group, and it was nearly three times that in irradiation control group. These data are shown in Figure 7 A.

DISCUSSION

The AuPPR synthesized in this study was small in size under the electron microscope. The average particle distribution radius measured with DLS was about 26.02 ± 0.744 nm. The small nanoparticle size makes it easier for the nanorods to enter cells through endocytosis [13]. The positive potential of AuNRs-PEI-PEG)/RGD (AuPPR) was 43.94 ± 6.95 mV. High positive potential makes the nanoparticles more stable and bind better to the negatively charged nucleic acids for entry into the cells [14]. Changes in zeta potential and UV absorption spectroscopy during the AuNRs characterization process demonstrate that different chemical groups were attached to the AuNR surface.

In the fluorescence transfection experiments, the transfection efficiency of AuNRs-PEI-PEG in combination with HIF-1α siRNA group (without RGD) was lower than that of AuPPR-HIF-1α siRNA group modified with RGD. The transfection efficiency of the experimental group, i.e., AuNRs-PEI-PEG without RGD, was only 42 ± 7. 9 %. The RGD polypeptide was specifically bound to the αvβ3 receptor, thereby enhancing endocytosis in the tumor cells [11]. For this reason, the transfection efficiency of AuPPR-HIF-1α siRNA group (84 ± 8.2 %) was higher than that of AuNRs-(PEI-PEG) group.

The results of cell cytotoxicity experiments indicated that the modified gold nanorod carrier complex (AuPPR) showed a significant decrease in biological toxicity, with AuNRs-CTAB being the most cytotoxic to cells. This may be due to the capacity of CTAB to destroy cell walls and precipitate polysaccharides. Therefore, AuNRs significantly reduced cytotoxicity after replacement of the superficial CTAB with thiol-containing MUA. In addition, PEG effectively reduced the toxic effects of pure PEI on cells [15]. Results showed that the cytotoxicity of gold nanocarrier complex modified by cationic copolymer (PEI-PEG)/RGD was decreased, nucleic acid-carrying capacity was enhanced, and the transfection efficiency was increased, which demonstrates good biocompatibility and practicability.

The combination of AuPPR and siRNA protected the siRNA from degradation outside the cell, prolonged its circulation in the body, and facilitated cell membrane penetration. Moreover, the PEI carrying nucleic acid had a unique "proton-sponging effect": on entering the cell, siRNA was released to exert the siRNA interference effect by acting on the corresponding targeted gene element. Therefore, the synthesized gold nanocarrier complex (AuPPR) was also a great nucleic acid carrier. The results of fluorescence transfection and western blotting also demonstrated that AuPPR efficiently carried the nucleic acid HIF-1αsiRN A into the cells.

Studies have shown that gold nanomaterials have radio-sensitization properties. Gold nanomaterials generate a large amount of reactive oxygen species (ROS) under photon irradiation, which causes DNA damage and apoptosis, thereby enhancing the susceptibility of cancer cells to irradiation therapy [16]. In the present work, it was observed that the AuPPR produced large amounts of ROS upon irradiation. Hence, there is good reason to believe that the main mechanism by which AuNRs-(PEI-PEG)/RGD increased the radio-sensitivity involved enhancement of ROS production resulting in increased cell damage.

Cell cycle distribution is considered to be one of the most important indices used to determine the degree of radio sensitivity of cells. Previous studies have shown that cells are most sensitive to irradiation in the G2/M phase, not so sensitive in the G1 phase, and least sensitive in the S phase. Therefore, it has also been suggested that part of the mechanism by which gold nanoparticles increase the radiosensitivity of tumor cells may be by inducing the conversion of hypoxic tumor cells to a more sensitive G2/M cycle. Furthermore, it has been reported that RGD also down-regulated the expression of the αvβ3 receptor on the surface of tumor cells and blocks the G2/M cell cycle, thereby increasing cell sensitivity to radiotherapy [17]. Changes in the cell cycle may partially explain the phenomenon of radiosensitivity observed in this study. However, the main mechanism is still considered to involve the increased production of ROS by gold nanorods.

The relative ROS content was significantly higher in simple AuPPR-irradiation group than in simple irradiation group. Some other studies have reported that low-energy photon radiation (MeV) of gold nanoparticles produced more secondary electrons and ROS than irradiation with high-energy grades (KeV). The radiosensitivity of cells at high energy level photon radiation is lower than that produced by low energy level photon radiation [18].

Based on the above theory, the AuPPR-HIF-1α siRNA2 group was introduced in this study, and it was shown that the AuPPR-HIF-1α siRNA2 very effectively increased the radiosensitivity of NPC hypoxia cells. Hypoxia of tumor cells is considered to be an important cause of cancer insensitivity to irradiation. Cancer cells are in hypoxic microenvironment during expansive growth. The HIF-1α and its downstream genes are activated and expressed in tumor cells under hypoxic microenvironment. These events promote cell DNA repair, reduce apoptosis and resist the killing of cells by radiation. The most effective siRNA sequence (HIF-1α siRNAa2) that interferes with HIF-1α expression was screened in this work, and it was demonstrated that AuPPR-HIF-1α siRNA2 effectively silenced HIF-1α protein expression.

The degree of apoptosis in the non-irradiation AuPPR-HIF-1α siRNA2 group was about twice as high as that of the normal control group. The above experimental results indicate that HIF-1α siRNA2 effectively silenced the expression of HIF-1α protein even in the non-irradiated condition, resulting in increased rate of apoptosis. The degree of apoptosis was about three times higher in AuPPR-HIF-1α siRNA2 irradiation group than in the normal irradiation group, and apoptosis was more evident in the simple AuPPR-irradiation group. In cell cycle studies, a sub-G1 peak was observed, which confirmed that a large number of cells had apoptosis and necrosis. These data suggest that AuPPR-HIF-1α siRNA2 significantly increased the sensitivity of tumors to radiotherapy.

This research has shown that both gold nanoparticles and AuPPR-HIF-1α siRNA2 exerted radio-sensitizing effects on hypoxic NPC cells. On one hand, gold nanoparticles generated high levels of ROS after X-ray exposure in tumor cells, which strengthened the DNA damage caused by radiation. On the other hand, AuPPR with HIF-1α siRNA significantly enhanced the radiotherapeutic effect on hypoxic tumor cells. When cancer cells are under hypoxia, HIF-1α siRNA down-regulates expressions of HIF-1α and its associated genes, weakens cancer cell adaptability to hypoxic conditions, inhibits tumor cell proliferation, and promotes apoptosis together with ROS produced by gold nanoparticles. These reasons greatly increase the susceptibility of hypoxic cancer cells to irradiation. However, the metabolism of NPs *in vitro*, and their targeting

mechanisms still need to be further studied. In addition, the association between AuNP-induced ROS and HIF-1α-controlled apoptotic signaling pathway requires further investigation.

CONCLUSION

Gold nanoparticles carrying HIF-1α siRNA are beneficial for increasing the radiotherapy/radiosensitivity of NPC. In the future, the study of gold nanomaterials and HIF-1 is expected to provide a wider range of research applications to solve the problem of radiation resistance of hypoxic tumor cells.

DECLARATIONS

Acknowledgements

None provided.

Funding

None provided.

Ethical approval

None provided.

Availability of data and materials

The datasets used and/or analyzed during the current study are available from the corresponding author on reasonable request.

Conflict of Interest

No conflict of interest associated with this work.

Contribution of Authors

We declare that this work was performed by the authors named in this article, and all liabilities pertaining to claims relating to the content of this article will be borne by the authors. Haosheng Zhang designed the study, supervised the data collection, and analyzed the data. Haosheng Zhang interpreted the data and prepared the manuscript for publication. Haosheng Zhang supervised the data collection, analyzed the data and reviewed the draft of the manuscript.

Open Access

REFERENCES

1. *Xu C, Chen YP, Ma J. Clinical trials in nasopharyngeal carcinoma-past, present and future. Chin Clin Oncol 2016; 5(2): 20.*
2. *Barker HE, Paget JT, Khan AA, Harrington KJ. The tumour microenvironment after radiotherapy: mechanisms of resistance and recurrence. Nat Rev Cancer 2015; 15(7): 409-425.*
3. *Balamurugan K. HIF-1 at the crossroads of hypoxia, inflammation, and cancer. Int J Cancer 2016; 138(5): 1058-1066.*
4. *Huang Y, Lin D, Taniguchi CM. Hypoxia-inducible factor (HIF) in the tumor microenvironment: friend or foe? Sci China Life Sci 2017; 60(10): 1114-1124.*
5. *Shim MS, Kwon YJ. Efficient and targeted delivery of siRNA in vivo. FEBS J 2010; 277(23): 4814-4827.*
6. *Ding Y, Jiang Z, Saha K, Kim CS, Kim ST, Landis RF, Rotello VM. Gold nanoparticles for nucleic acid delivery. Mol Ther 2014; 22(6): 1075-1083.*
7. *Choi BJ, Jung KO, Graves EE, Pratx G. A gold nanoparticle system for the enhancement of radiotherapy and simultaneous monitoring of reactive-oxygen-species formation. Nanotechnol 2018; 29(50): 504001.*
8. *Hainfeld JF, Slatkin DN, Smilowitz HM. The use of gold nanoparticles to enhance radiotherapy in mice. Phys Med Biol 2004; 49(18): N309-15.*
9. *Chang Y, He L, Li Z, Zeng L, Song Z, Li P, Chan L, You Y, Yu XF, Chu PK, Chen T. Designing core-shell gold and selenium nanocomposites for cancer radiochemotherapy. ACS Nano 2017; 11(5): 4848-4858.*
10. *Pinnapireddy SR, Duse L, Strehlow B, Schäfer J, Bakowsky U. Composite liposome-PEI/nucleic acid lipopolyplexes for safe and efficient gene delivery and gene knockdown. Colloids Surf B Biointerfaces 2017; 158: 93-101.*
11. *Shan D, Li J, Cai P, Prasad P, Liu F, Rauth AM, Wu XY. RGD-conjugated solid lipid nanoparticles inhibit adhesion and invasion of αvβ3 integrin-overexpressing breast cancer cells. Drug Deliv Transl Res 2015; 5(1): 15-26.*
12. *Chuang CC, Cheng CC, Chen PY, Lo C, Chen YN, Shih MH, Chang CW. Gold nanorod-encapsulated biodegradable polymeric matrix for combined photothermal and chemo-cancer therapy. Int J Nanomedicine 2018; 14: 181-193.*
13. *Danhier F. To exploit the tumor microenvironment: Since the EPR effect fails in the clinic, what is the future of nanomedicine? J Cont Rel 2016; 244(Pt A): 108-121.*

14. Nakatsuji H, Kawabata Galbraith K, Kurisu J, Imahori H, Murakami T, Kengaku M. Surface chemistry for cytosolic gene delivery and photothermal transgene expression by gold nanorods. Sci Rep 2017; 7(1): 4694.
15. Amani A, Kabiri T, Shafiee S, Hamidi A. Preparation and characterization of PLA-PEG-PLA/PEI/DNA nanoparticles for improvement of transfection efficiency and controlled release of DNA in gene delivery systems. Iran J Pharm Res 2019; 18(1): 125-141.
16. Her S, Jaffray DA, Allen C. Gold nanoparticles for applications in cancer radiotherapy: Mechanisms and recent advancements. Adv Drug Deliv Rev 2017; 109: 84-101
17. Xu W, Luo T, Li P, Zhou C, Cui D, Pang B, Ren Q, Fu S. RGD-conjugated gold nanorods induce radiosensitization in melanoma cancer cells by downregulating $\alpha(v)\beta_3$ expression. Int J Nanomed 2012; 7: 915-24.
18. Douglass M, Bezak E, Penfold S. Monte Carlo investigation of the increased radiation deposition due to gold nanoparticles using kilovoltage and megavoltage photons in a 3D randomized cell model. Med Phys 2013; 40(7): 071710.